Thermal Decomposition Behavior of Carbon-Nanotube-Reinforced Poly(ethylene 2,6-naphthalate) Nanocomposites

Jun Young Kim,[1]* Hawe Soo Park,[2] Seong Hun Kim[2]

[1]*Material Laboratory, Corporate R&D Center, Samsung SDI Company, Limited, 575 Shin-dong, Yeongtong-gu, Suwon-si, Gyeonggi-do, 443-731 Republic of Korea*
[2]*Department of Fiber and Polymer Engineering, Hanyang University, 17 Haengdang-dong, Seongdong-gu, Seoul, 133-791 Republic of Korea*

Received 16 November 2008; accepted 17 February 2009
DOI 10.1002/app.30297
Published online 17 April 2009 in Wiley InterScience (www.interscience.wiley.com).

ABSTRACT: Polymer nanocomposites based on poly (ethylene 2,6-naphthalate) (PEN) and carbon nanotubes (CNTs) were prepared by direct melt blending with a twin-screw extruder. Dynamic thermogravimetric analysis was conducted on the PEN/CNT nanocomposites to clarify the effect of CNTs on the thermal decomposition behavior of the polymer nanocomposites. The thermal decomposition kinetics of the PEN/CNT nanocomposites was strongly dependent on the CNT content, the heating rate, and the gas atmosphere. On the basis of the thermal decomposition kinetic analysis, the variation of the activation energy for thermal decomposition revealed that a very small quantity of CNTs substantially improved the thermal stability and thermal decomposition of the PEN/CNT nanocomposites. Morphological observations demonstrated the formation of interconnected or network-like structures of CNTs in the PEN matrix. The unique character of the CNTs introduced into the PEN matrix, such as the physical barrier effect of CNTs during thermal decomposition and the formation of interconnected or network-like structures of CNTs, resulted in the enhancement of the thermal stability of the PEN/CNT nanocomposites. © 2009 Wiley Periodicals, Inc. J Appl Polym Sci 113: 2008–2017, 2009

Key words: blends; nanocomposites; thermogravimetric analysis (TGA)

INTRODUCTION

Polymer nanocomposites based on the reinforcement of polymers with nanofillers have attracted a great deal of interest in fields ranging from the scientific to the industrial because of remarkable improvements in the physical properties at lower filler loadings. The fabrication of polymer nanocomposites reinforced with various nanofillers is believed to be a key technology for advanced composite materials. Among various nanofillers, carbon nanotubes (CNTs) are regarded as promising reinforcements in polymer nanocomposites because of their combination of uniquely excellent properties with a high aspect ratio and a small size.[1–3] This feature has motivated a number of efforts to fabricate polymer/CNT nanocomposites in the development of next-generation high-performance polymeric materials, and much research has been conducted on the practical realization of the extraordinary properties of CNTs for advanced nanocomposites in a broad range of industrial applications. However, because of the high cost and limited availability, only a few practical applications in industrial fields, such as electronic and electric appliances, have been realized to date.

Poly(ethylene 2,6-naphthalate) (PEN) is a transparent aromatic polyester that has been widely used in conventional industry, and it is of great industrial importance because of its high performance, good physical properties, and low cost. In general, PEN, having naphthalene rings in its main chains, exhibits enhanced mechanical, thermal, and gas barrier properties in comparison with other polyesters. Thus, PEN has potential for industrial applications such as high-performance industrial fibers, magnetic tape, food packaging materials, and flexible printed circuits. In this respect, extensive research has been conducted for the development of commercial applications of PEN, such as high-performance polymers.[4–7] Although PEN is promising, its insufficient thermal stability and physical properties have often hindered practical applications in a broad range of industries.

The thermal stability of polymers plays a crucial role in determining their processing and applications because it affects the final properties of polymers, such as the upper limit use temperature and

**Present address:* Department of Materials Science and Engineering, Massachusetts Institute of Technology, Cambridge, Massachusetts.

Correspondence to: J. Y. Kim (junykim74@hanmail.net) and S. H. Kim (kimsh@hanyang.ac.kr).

dimensional stability. For the fabrication of polymer composites with better balance in processing and performance, it is very instructive to characterize the thermal stability and decomposition kinetics of polymer composites. Thus, an understanding of the thermal decomposition behavior of polymer nanocomposites makes it possible to develop commercial applications in a broad range of industries. Up to now, most research on polymer/CNT nanocomposites has focused on their preparation, crystallization behavior, morphology, rheological behavior, and mechanical properties.[8–16] Although PEN has potential for industrial applications, such as high-performance polymers and industrial fibers, the thermal stability and thermal decomposition kinetics of PEN/CNT nanocomposites have been rarely investigated to date. In addition, the combination of a small quantity of expensive CNTs with cheap conventional polyester resins provides an attractive possibility for improving the thermal stability and physical properties of polymer/CNT nanocomposites at a low processing cost from an industrial perspective.[11–16]

In this study, polymer nanocomposites based on PEN and a small quantity of CNTs were prepared by simple melt blending in a twin-screw extruder in an effort to create high-performance polymer composites with a cost-effective method for possible applications in a wide range of industries. The effects of CNTs on the thermal stability, thermal decomposition behavior, and physical properties of PEN/CNT nanocomposites are discussed. We expect that this study will help with the preliminary evaluation and understanding of their thermal stability and decomposition behavior. Our study suggests a simple and cost-effective method that will facilitate the industrial realization of PEN/CNT nanocomposites with enhanced thermal stability.

EXPERIMENTAL

Materials and preparation of the nanocomposites

The conventional thermoplastic polymer PEN, with an intrinsic viscosity of 0.97 dL/g, was supplied by Hyo Sung Corp. (Korea). The nanotubes were multiwalled CNTs (degree of purity >95%) synthesized by a thermal chemical vapor deposition process; they were purchased from Iljin Nanotech Co. (Korea). The length and diameter of the CNTs were in the ranges of 10–50 μm and 10–30 nm, respectively, and this indicated that their aspect ratio reached 1000.

All materials were dried at 120°C *in vacuo* for 24 h before use to minimize the effects of moisture. PEN/CNT nanocomposites were prepared by a melt-blending process in a Haake rheometer (Haake Technik GmbH, Germany) equipped with a twin screw. The temperatures of the heating zone, from the hopper to the die, were set to 280, 290, 295, and 285°C, and the screw speed was fixed at 20 rpm. For the fabrication of PEN/CNT nanocomposites, PEN was melt-blended with CNTs at the specific concentration of 0.5, 1.0, or 2.0 wt % in the PEN matrix. Upon the completion of melt blending, extruded strands were allowed to cool in the water bath and then cut into pellets with a constant diameter and length with a PP1 rate-controlled pelletizer (Haake Technik).

Characterization

Thermogravimetric analysis (TGA) of PEN/CNT nanocomposites was performed with a TA Instrument SDF-2960 thermogravimetric analyzer over the temperature range of 30–800°C under nitrogen and air with a flow rate of 30 mL/min. Dynamic TGA measurements for PEN/CNT nanocomposites were performed at heating rates of 5, 10, and 20°C/min. The morphology of PEN/CNT nanocomposites was observed with a JEOL JSM-6340F scanning electron microscope with an accelerating voltage of 15 kV. Dynamic mechanical properties of PEN/CNT nanocomposites were measured with a TA Instrument Q-800 dynamic mechanical thermal analyzer in a tensile mode at a fixed frequency of 1 Hz over the temperature range of 30–250°C at a heating rate of 5°C/min.

RESULTS AND DISCUSSION

Thermal stability

The thermal stability of polymer composites determines the upper limit of the working temperature and the environmental conditions for use; these are related to the thermal decomposition temperature, the thermal decomposition rate, and the thermal decomposition kinetics.[17] TGA thermograms of PEN/CNT nanocomposites with the CNT content at 20°C/min under nitrogen are shown in Figure 1, and their results are summarized in Table I. The TGA curves of thermal decomposition for pure PEN and PEN/CNT nanocomposites exhibited only one primary weight-loss step during thermal decomposition, which was attributed to the random scission of the PEN macromolecular chains.[18] In addition, the pattern of TGA curves for PEN/CNT nanocomposites was similar to that of pure PEN, suggesting that the thermal decomposition of PEN/CNT nanocomposites may mostly stem from PEN. The incorporation of CNTs into the PEN matrix increased the thermal decomposition temperatures and residual yields of PEN/CNT nanocomposites, and this enhancing effect was more pronounced at high CNT contents. This result indicated that the introduction of CNTs could lead to the stabilization of PEN,

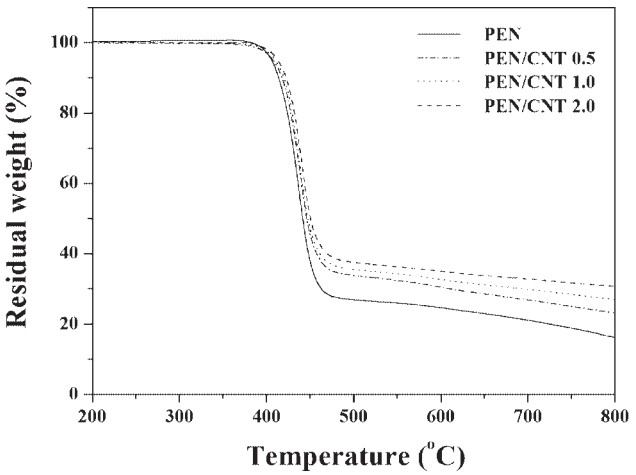

Figure 1 TGA thermograms of PEN/CNT nanocomposites with the CNT content under a nitrogen atmosphere.

resulting in the enhancement of the thermal stability of PEN/CNT nanocomposites. The thermal decomposition temperatures and decomposition kinetic parameters, including the initial decomposition temperature [at 5 (T_5) or 10% (T_{10}) weight loss], the integral procedure decomposition temperature (IPDT), the temperature at the maximum rate of weight loss [i.e., the absolute temperature at the maximum rate of thermal decomposition (T_{dm}); see eq. (7)], and the activation energy for thermal decomposition (E_a), are in common use for estimating the thermal stability of polymers and polymer composites.[19] As shown in Table I, the thermal stability factors [including T_5, T_{10}, T_{dm}, the area ratio of the total experimental curve divided by the total TGA thermograms (A), the coefficient of A (K), and IPDT] of the PEN/CNT nanocomposites were higher than those of pure PEN, and this enhancing effect was more pronounced at higher CNT contents. This feature resulted from the good thermal stability and heat resistance of CNTs, which retarded the rate of thermal decomposition of PEN/CNT nanocomposites, contributing to the increase in the thermal stability factors of PEN/CNT nanocomposites. In addition, the residual yields of PEN/CNT nanocomposites increased with increasing CNT content, and this implied that PEN molecular chains were more difficult to decompose in the presence of CNTs. The presence of CNTs could enhance the thermal stability of PEN/CNT nanocomposites and retard thermal volatilization during thermal decomposition.

TGA thermograms of the PEN/CNT 2.0 nanocomposites at various heating rates under nitrogen and air are shown in Figure 2. TGA curves of PEN/CNT nanocomposites shifted toward higher temperature regions with increasing heating rates. This behavior may be explained by the fact that polymer molecules did not have enough time to exhaust heat energy with the heating rate increasing, and this led to a slower decomposition rate and a higher decomposition temperature because of the slow diffusion of heat.[20] As shown in Figure 2(b), TGA curves of PEN/CNT nanocomposites exhibited two weight-loss stages during thermal decomposition under air. For instance, PEN/CNT 2.0 nanocomposites exhibited the first weight-loss step of thermal decomposition between 380 and 475°C with $T_{dm} = 444$°C under air, and this was similar to what was observed under nitrogen. The second weight-loss step of thermal decomposition of PEN/CNT 2.0 nanocomposites under air was observed between 475 and 600°C with $T_{dm} = 551$°C, and this was not observed under nitrogen. The first weight-loss step was attributed to the thermal degradation of PEN from high-molecular-weight macromolecules to small fragments due to the random scission of polymer chains,[18] whereas the second weight-loss step resulted from thermo-oxidative decomposition of degraded smaller chain fragments into volatile products under air.[21] This result revealed that there was a dependence of the thermal decomposition of PEN/CNT nanocomposites on the gas atmosphere during dynamic TGA measurements. TGA results for PEN/CNT nanocomposites with the CNT content and heating under air are shown in Table II. As observed under nitrogen, the incorporation of CNTs into the PEN matrix increased the thermal decomposition temperatures and residual yields of PEN/CNT nanocomposites, and this enhancing effect was more pronounced at higher CNT contents. The increase in the thermal decomposition temperatures of PEN/CNT nanocomposites with increasing CNT content may be explained by the fact that the introduced CNTs

TABLE I
Effect of CNTs on the Thermal Stability of PEN/CNT Nanocomposites

Material	T_5 (°C)	T_{10} (°C)	T_{dm} (°C)	A	K	IPDT (°C)	W_R (%)
PEN	406.5	417.3	436.8	0.636	1.340	686.5	14.8
PEN/CNT 0.5	409.9	420.2	438.7	0.663	1.531	812.1	22.7
PEN/CNT 1.0	410.3	421.9	439.8	0.677	1.661	896.2	26.9
PEN/CNT 2.0	411.9	422.5	440.9	0.690	1.793	982.9	30.3

IPDT $= A \times K(T_f - T_i) + T_i$;[19] T_f = final experimental temperature; T_i = initial experimental temperature; W_R = residual yield in a TGA thermogram at 800°C under N_2.

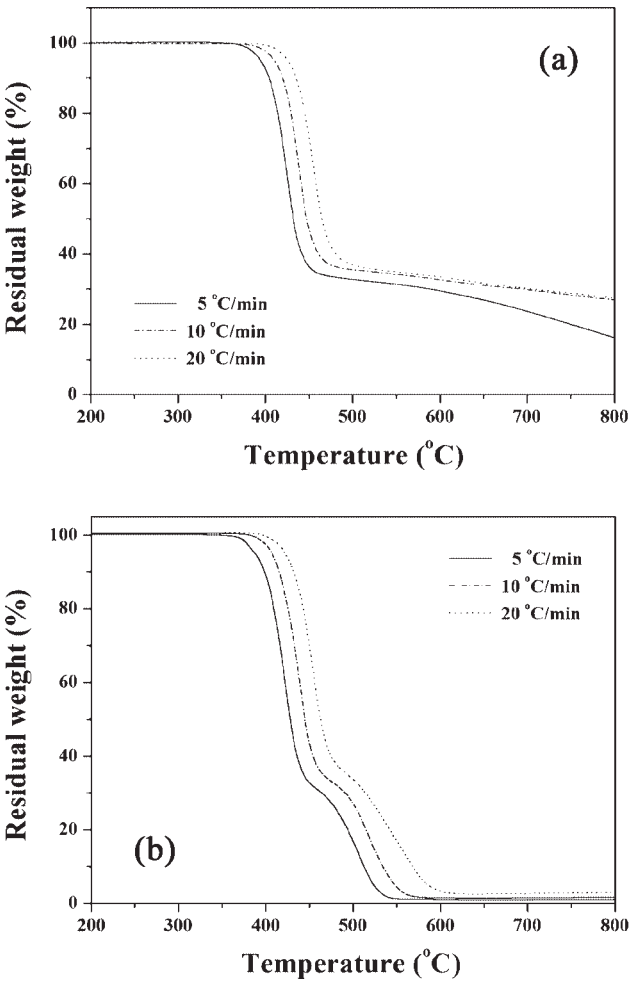

Figure 2 TGA thermograms of PEN/CNT 2.0 nanocomposites at various heating rates under (a) nitrogen and (b) air atmospheres.

can effectively act as physical barriers to prevent the transport of volatile decomposed products out of PEN/CNT nanocomposites during thermal decomposition,[22] resulting in the enhancement of the thermal stability of PEN/CNT nanocomposites. In addition, the residual yields of PEN/CNT nanocomposites under air were lower than those under N_2, and this was attributed to the fact that the formation of smaller fragmented products in the nanocomposites by oxidation occurred easily under air.

In PEN/CNT nanocomposites, the incorporated CNTs could induce protective barriers against thermal decomposition and retard the thermal decomposition of PEN/CNT nanocomposites; this resulted from the physical barrier effects of the incorporated nanofillers, which acted as mass and heat transfer barriers.[22–24] Consequently, the thermal stability of PEN/CNT nanocomposites was significantly improved with the introduction of a small quantity of CNTs. A similar effect was previously reported: CNT layers exhibited a good barrier effect on gases such as oxygen and nitrogen and could not only insulate polymers but also reduce the weight-loss rate of decomposed products, resulting in an improvement in the thermal stability and flame retardancy of polymer nanocomposites.[22] Bocchini et al.[25] reported that for CNTs and linear low-density polyethylene (LLDPE) nanocomposites, the presence of CNTs delayed thermooxidative degradation in an air atmosphere. They suggested that the stabilization of the LLDPE matrix was attributable to the formation of a thin protective film consisting of CNTs and polyaromatic carbon char generated on the surface of LLDPE/CNT nanocomposites during thermal degradation, and this protective film prevented the diffusion of oxygen toward the polymer matrix and the development of volatile decomposed products in the polymer nanocomposites, resulting in the enhancement of the thermal stability of LLDPE/CNT nanocomposites under thermooxidative

TABLE II
TGA Results for PEN/CNT Nanocomposites with the CNT Content and Heating Rate Under an Air Atmosphere

Material	Heating rate (°C/min)	T_5 (°C)	T_{10} (°C)	T_{60} (°C)	T_{dm1} (°C)	T_{dm2} (°C)	W_R (%)
PEN	5	387.9	398.7	434.2	421.1	506.8	0.2
	10	402.2	412.4	454.4	439.6	517.2	0.7
	20	420.2	430.4	467.8	455.2	540.7	1.4
PEN/CNT 0.5	5	390.9	399.5	436.0	423.0	512.8	1.1
	10	406.9	415.5	459.5	440.6	544.8	1.2
	20	421.4	432.2	474.8	456.6	555.2	1.5
PEN/CNT 1.0	5	392.1	401.9	451.2	423.1	518.8	1.6
	10	407.2	416.8	460.2	441.8	548.7	1.7
	20	422.2	432.3	475.8	457.3	560.3	2.6
PEN/CNT 2.0	5	393.0	403.3	456.9	428.9	535.6	2.4
	10	408.2	417.6	467.8	444.4	551.7	3.0
	20	423.7	432.9	476.7	457.8	563.6	3.8

T_{60} = decomposition temperature at 60% weight loss; T_{dm1} = maximum decomposition temperature in the first stage; T_{dm2} = maximum decomposition temperature in the second stage; W_R = residual yield in a TGA thermogram at 800°C under air.

conditions. In addition, Hsu et al.[26] reported that CNTs interrupted chain propagation because of their strong radical-accepting capacity,[27] leading to antioxidant effects in polymers during the thermal decomposition process. Therefore, the retardation of the thermal decomposition of PEN/CNT nanocomposites with the introduction of CNTs may be attributed to the physical barrier effect promoted by the dispersed CNTs as effective thermal insulators and protective layers in PEN/CNT nanocomposites; this suggests that a small quantity of CNTs was beneficial, with the CNTs acting as efficient decomposition-resistant nanoreinforcing fillers in PEN/CNT nanocomposites.

Thermal decomposition kinetics

In the thermal decomposition process of a polymer,[28] the degree of thermal decomposition or conversion (α) can be calculated as follows:

$$\alpha = \frac{W_0 - W_t}{W_0 - W_f} \tag{1}$$

where W_t, W_0, and W_f are the actual, initial, and final weights of the samples, respectively. If it is assumed that the rate of conversion is a linear function of a temperature-dependent rate constant [$K(T)$] and a temperature-independent/weight-loss-dependent function [$F(\alpha)$], the rate of decomposition can be expressed as follows:

$$\frac{d\alpha}{dt} = K(T)F(\alpha) \tag{2}$$

where t and T are the reaction time and temperature, respectively, and $F(\alpha) = (1 - \alpha)^n$ depends on the mechanism of the thermal decomposition reaction. The function $K(T)$ can be described by the Arrhenius equation as follows:

$$K(T) = a\exp\left(\frac{-E_a}{RT}\right) \tag{3}$$

where a is the pre-exponential factor and R is the universal gas constant. At a constant heating rate ($\beta = dT/dt$), the basic equation for the thermal decomposition kinetics can be expressed in terms of the combination of eqs. (2) and (3) as follows:

$$\frac{d\alpha}{dt} = \left(\frac{a}{\beta}\right)\exp\left(\frac{-E_a}{RT}\right)F(\alpha) \tag{4}$$

Using this equation, theoretical approaches, based on the differential mode and integral mode, were applied for the estimation of the thermal decomposition kinetic parameters.[29–31]

The Flynn–Wall–Ozawa method[32] has been used to determine E_a from dynamic tests via the plotting of the logarithm of the heating rate as a function of the inverse of the temperature at different conversions. Being integrated with the initial condition of $\alpha = 0$ at $T = T_0$, eq. (4) can be arranged as follows:

$$F(\alpha) = \left(\frac{a}{\beta}\right)\int_0^T \exp\left(\frac{-E_a}{RT}\right)dT \tag{5}$$

Then, with Doyle's approximation,[33] eq. (5) can be simplified as follows:

$$\log\beta = \log\left(\frac{a \cdot E_a}{F(\alpha)R}\right) - 2.315 - 0.4567\left(\frac{E_a}{RT}\right) \tag{6}$$

E_a for a specific weight loss can be calculated from the slope of the plot of log β versus $1/T$.

Kissinger's method[29] has been used to estimate E_a; it involves the maximum temperature of the first-derivative weight-loss curves in TGA measurements at a constant heating rate. The Kim–Park method[34] has been used to determine E_a from TG and derivative thermogravimetry (DTG) thermograms at various heating rates; the logarithm of the heating rate is plotted as a function of the inverse of T_{dm}. The resulting equations can be expressed as follows:

$$\ln\left(\frac{\beta}{T_{dm}^2}\right) = \left[\ln\left(\frac{ZR}{E_a}\right) - \ln F(\alpha)\right] - \left(\frac{E_a}{RT_{dm}}\right) \tag{7}$$

$$\ln\beta = \ln Z + \ln\left(\frac{E_a}{R}\right) + \ln\left[1 - n + \left(\frac{n}{0.944}\right)\right] - 5.3305 - 1.0516\left(\frac{E_a}{RT_{dm}}\right) \tag{8}$$

where Z is the frequency factor and n is the reaction order. E_a can be calculated from the slopes of the plots of $\ln(\beta/T_{dm}^2)$ versus $1/T_{dm}$ and $\ln\beta$ versus $1/T_{dm}$, respectively.

E_a

On the basis of the data obtained from TGA thermograms at different heating rates, plots of log β versus $1/T$ for PEN/CNT nanocomposites under N_2 and air are shown in Figure 3. The Flynn–Wall–Ozawa plots of PEN/CNT nanocomposites exhibited a good linear relationship, and this indicated that the Flynn–Wall–Ozawa analysis was effective in describing the thermal decomposition kinetics of PEN/CNT nanocomposites. The thermal decomposition of PEN/CNT nanocomposites may vary with the degree of thermal decomposition under N_2 and air. The E_a values of PEN/CNT nanocomposites under N_2 and air, estimated from the slopes of the Flynn–Wall–Ozawa plots, are shown in Table III. The variations of the E_a values with the weight loss observed

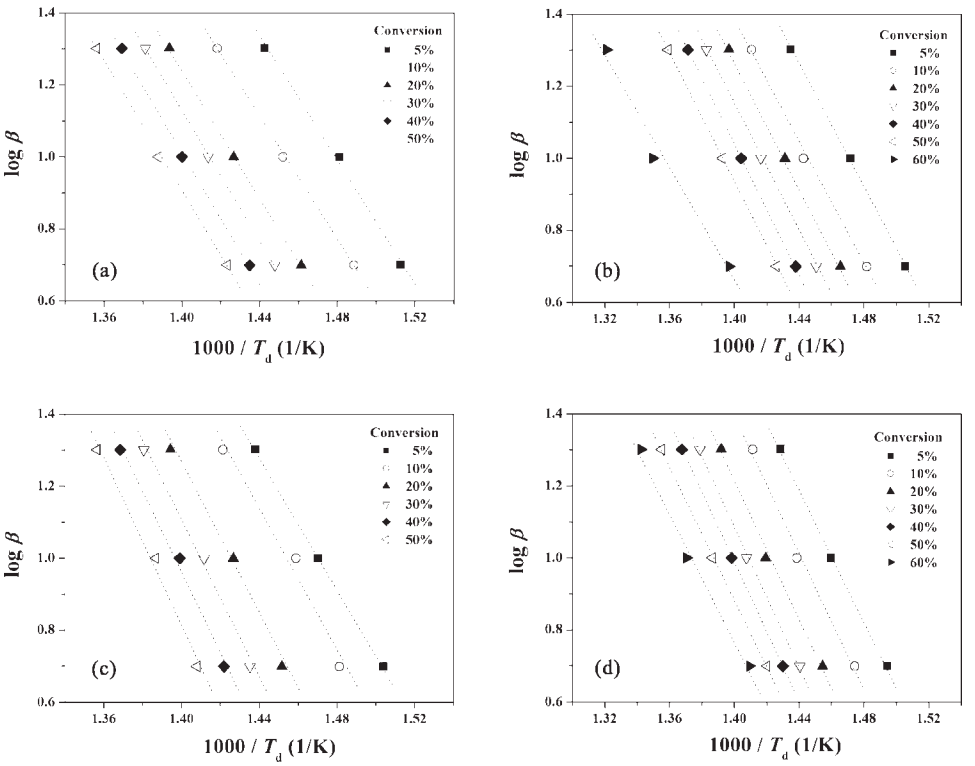

Figure 3 Flynn-Wall-Ozawa plots of PEN/CNT nanocomposites: (a) PEN under nitrogen, (b) PEN under air, (c) PEN/CNT 2.0 under nitrogen, and (d) PEN/CNT 2.0 under an air atmosphere. With eq. (6), the slope of the plot of log β versus $1/T_d$ (where T_d is the decomposition temperature) provides an estimate of E_a for PEN/CNT nanocomposites.

in PEN/CNT nanocomposites indicated the variation in the thermal decomposition. The E_a values of PEN/CNT nanocomposites were higher than those of pure PEN, and they tended to increase with the CNT content. In general, a higher E_a value reflects better thermal stability of polymer composites.[25] The increase in the E_a values of PEN/CNT nanocomposites with increasing CNT content indicated that the thermal decomposition of PEN/CNT nanocomposites was more difficult at higher CNT contents. As shown in Table III, the E_a values of PEN/CNT nanocomposites were lower under air than those under N_2, and this indicated that PEN/CNT nanocomposites exhibited faster thermal decomposition kinetics

TABLE III
E_a and r^2 Values of PEN/CNT Nanocomposites by the Flynn–Wall–Ozawa Method

Degree of decomposition (%)	PEN		PEN/CNT 0.5		PEN/CNT 1.0		PEN/CNT 2.0	
	E_a (kJ/mol)	r^2	E_a (kJ/mol)	r^2	E_a (kJ/mol)	r^2	E_a (kJ/mol)	r^2
Under nitrogen								
5	156.6	0.998	164.1	0.999	166.5	1.000	167.0	1.000
10	155.9	0.999	163.6	1.000	175.5	1.000	179.2	0.989
20	161.2	1.000	162.7	0.998	177.1	0.992	189.7	0.997
30	164.3	0.999	164.6	0.999	172.9	0.996	199.4	0.996
40	166.4	0.999	170.8	1.000	172.3	0.997	203.6	0.996
50	163.5	0.999	172.0	0.996	182.0	1.000	211.5	0.994
Average	161.3		166.3		174.4		191.7	
Under air								
5	155.3	0.999	163.0	0.998	165.9	1.000	166.7	0.999
10	153.4	0.998	158.3	0.998	167.9	0.996	172.7	0.996
20	158.7	1.000	160.1	0.999	169.3	0.998	173.8	0.997
30	161.2	1.000	165.0	0.999	169.0	0.999	176.9	0.999
40	164.6	1.000	166.7	0.999	169.4	0.999	175.6	1.000
50	163.6	1.000	166.2	0.999	167.8	0.999	168.3	0.999
60	141.8	0.990	145.6	1.000	153.3	1.000	161.9	0.995
Average	156.9		160.7		166.1		170.8	

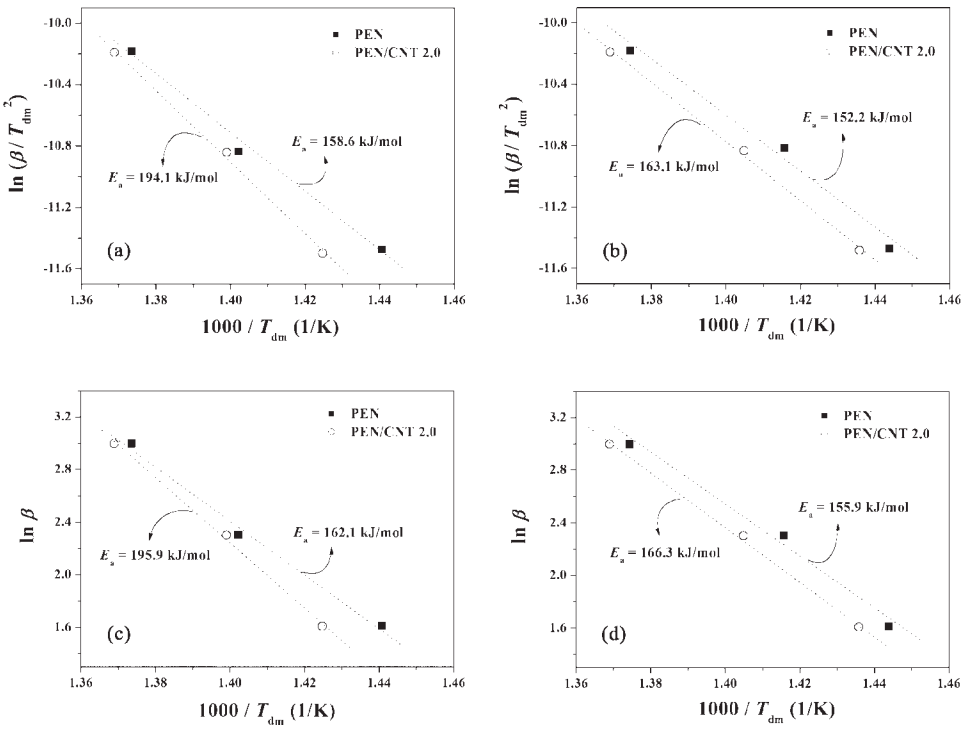

Figure 4 Kissinger and Kim–Park plots of PEN/CNT nanocomposites under (a,c) nitrogen and (b,d) air atmospheres. With eqs. (7) and (8), the slopes of the plots of $\log(\beta/T_{dm}^2)$ versus $1/T_{dm}$ and ln β versus $1/T_{dm}$ provide estimates of E_a for PEN/CNT nanocomposites.

and lower thermal stability under air versus N_2. The occurrence of the thermooxidative reaction by the active effect of oxygen under an air atmosphere could lead to an increase in the decomposition rate, resulting in the acceleration of the thermal decomposition of PEN/CNT nanocomposites. This result demonstrated that the incorporation of CNTs into the PEN matrix had a significant effect on the thermal stability and thermal decomposition kinetics of PEN/CNT nanocomposites. In addition, it can be deduced that the E_a values of PEN/CNT nanocomposites calculated with the Flynn–Wall–Ozawa method exhibited good reliability in describing the thermal decomposition kinetics of PEN/CNT nanocomposites; this was confirmed by the fact that the values of the correlation coefficient (r^2) were greater than 0.99.

Based on dynamic TGA data obtained from TGA thermograms at different heating rates, the Kissinger and Kim–Park plots of PEN/CNT nanocomposites are shown in Figure 4. The Kissinger and Kim–Park plots of PEN/CNT nanocomposites exhibited a good linear relationship, and this indicated that the Kissinger and Kim–Park analyses were effective in describing the thermal decomposition kinetics of PEN/CNT nanocomposites. The E_a values of PEN/CNT nanocomposites were higher than those of pure PEN, and they tended to increase with increasing CNT content; this indicated that the thermal decomposition of PEN/CNT nanocomposites was more difficult at higher CNT contents. As shown in Table IV, PEN/CNT nanocomposites exhibited higher E_a values under N_2 than under air. This feature may be explained by the fact that the

TABLE IV
E_a and r^2 Values of PEN/CNT Nanocomposites by the Kissinger and Kim–Park Methods

	Kissinger method				Kim–Park method			
	Under nitrogen		Under air		Under nitrogen		Under air	
Material	E_a (kJ/mol)	r^2	E_a (kJ/mol)	r^2	E_a (kJ/mol)	r^2	E_a (kJ/mol)	r^2
PEN	158.6	0.996	152.2	0.993	162.1	0.996	155.9	0.993
PEN/CNT 0.5	159.4	0.998	160.2	0.998	162.8	0.998	163.6	0.999
PEN/CNT 1.0	167.0	0.997	160.5	0.993	170.1	0.997	163.8	0.995
PEN/CNT 2.0	194.1	0.998	163.1	0.994	195.9	0.999	166.3	0.994

thermooxidative reactions under an air atmosphere increased the decomposition rate, leading to the acceleration of thermal decomposition for PEN/CNT nanocomposites. According to a comparison of the two methods, the E_a values obtained with the Kissinger method were slightly smaller than those obtained with the Kim–Park method, whereas the two methods revealed similar trends for the E_a values with the introduction of CNTs. This tendency was in accordance with the results obtained from the Flynn–Wall–Ozawa analysis. In addition, it can be deduced that the E_a values of PEN/CNT nanocomposites calculated with the Kissinger method exhibited good reliability in describing the thermal decomposition of PEN/CNT nanocomposites; this was confirmed by the fact that the values of r^2 were greater than 0.99.

Although the actual E_a values were affected by various factors such as the calculation method of the kinetic parameters, the mass and size of the samples, the gas atmosphere, and the operating conditions,[35–37] the three kinetic analyses employed in this study exhibited good applicability to the thermal decomposition kinetics of PEN/CNT nanocomposites. As shown in Tables III and IV, the variation of the E_a values of PEN/CNT nanocomposites with the applied methods and atmospheres indicates that there is a dependence of the thermal decomposition kinetics for PEN/CNT nanocomposites on the estimation method and the employed atmosphere. On the basis of the variations of the E_a values, the thermal decomposition process of PEN/CNT nanocomposites under air may be attributed to the combined effect of thermal pyrolytic kinetics and thermooxidative decomposition kinetics.[38] Dynamic TGA kinetic analysis of PEN/CNT nanocomposites demonstrated that the incorporation of CNTs into the PEN matrix increased the E_a values of PEN/CNT nanocomposites, and this was related to the enhancement of the thermal stability of PEN/CNT nanocomposites. In PEN/CNT nanocomposites, the introduced CNTs effectively acted as physical barriers, inducing the retardation of thermal decomposition and preventing the transport of volatile degraded products out of the polymer nanocomposites during thermal decomposition.[22] Thus, the thermal stability of PEN/CNT nanocomposites was enhanced by the physical barrier effect of CNTs against thermal decomposition, and this led to higher E_a values of PEN/CNT nanocomposites in comparison with pure PEN.

Morphology

The morphologies of the PEN/CNT 2.0 nanocomposites and the residues after thermal decomposition under nitrogen are shown in Figure 5. For PEN/CNT nanocomposites, CNTs were randomly dispersed in the PEN matrix, and their interconnected or network-like structures were formed in the PEN matrix through nanotube–nanotube or nanotube–polymer interactions.[12] The CNTs with a small size, a high aspect ratio, and a large surface area were often subjected to self-agglomeration or bundle formation at higher CNT contents and thus easily formed the interconnected or network-like structures in the molten polymer matrix. After the thermal decomposition process, the introduced CNTs still kept the interconnected network-like structures in the PEN matrix, despite some collapse or loss of their form, as shown in Figure 5(b). This morphological feature of the CNTs dispersed in the PEN matrix might be another possible reason for the enhanced thermal stability of PEN/CNT nanocomposites because the interconnected network structures

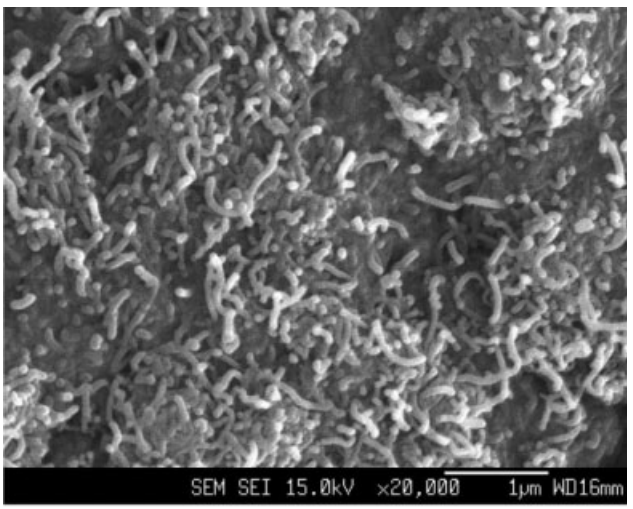

Figure 5 Scanning electron microscopy images of (a) PEN/CNT 2.0 nanocomposites and (b) their residues after thermal decomposition under nitrogen.

induced by CNTs in the PEN matrix resulted in a good physical barrier effect against the thermal decomposition of PEN/CNT nanocomposites by retarding the thermal decomposition of the polymer nanocomposites and by acting as protective layers on the PEN matrix. A similar observation was reported by Schartel et al.[39] for polyamide (PA)/CNT nanocomposites: the increased viscosity of PA/CNT nanocomposites and the fiber-network character of the incorporated CNTs were the dominant mechanisms influencing the fire retardancy of PA/CNT nanocomposites, and this suggested that the interconnected network structures of CNTs stabilized the melt in the pyrolysis zone and residue. In PEN/CNT nanocomposites, the incorporation of CNTs into the PEN matrix could enhance the thermal stability of PEN/CNT nanocomposites, leading to the increase in E_a. This enhancing effect of CNTs on the thermal stability and thermal decomposition of PEN/CNT nanocomposites may also be explained by the high thermal stability of CNTs and the restriction of macromolecular chains by the presence of CNTs.[40] In addition, the increased thermal conductivity of PEN/CNT nanocomposites due to the excellent thermal conductivity of CNTs[41] could lead to effective heat dissipation with PEN/CNT nanocomposites,[42] resulting in an enhancement of the thermal stability of PEN/CNT nanocomposites.

Dynamic mechanical properties

The dynamic mechanical properties of PEN/CNT nanocomposites as a function of temperature are shown in Figure 6(a). There was a significant dependence of the storage modulus (E') and loss tangent (tan δ) of PEN/CNT nanocomposites on the temperature and the presence of CNTs. As molecular motions within the polymers changed, the modulus of the polymers varied with the temperature. E' of the polymers decreased rapidly, whereas tan δ underwent a maximum when the polymers were heated through the glass-transition region. The apparent glass-transition region was revealed by a rapid decrease in E' of PEN/CNT nanocomposites. The incorporation of a small quantity of CNTs into the PEN matrix increased E' of PEN/CNT nanocomposites, and this was attributed to the physical interactions between the PEN matrix and the CNTs with a high aspect ratio and a large surface area and to the stiffening effect of CNTs as nanoreinforcing fillers, which provided the capability to allow an efficient load transfer in PEN/CNT nanocomposites. In addition, the peak position of tan δ for PEN/CNT nanocomposites was not affected by the presence of CNTs, whereas the peak height decreased. For characterizing the effect of CNTs on the ability to sustain the modulus with increasing temperature, the ratio

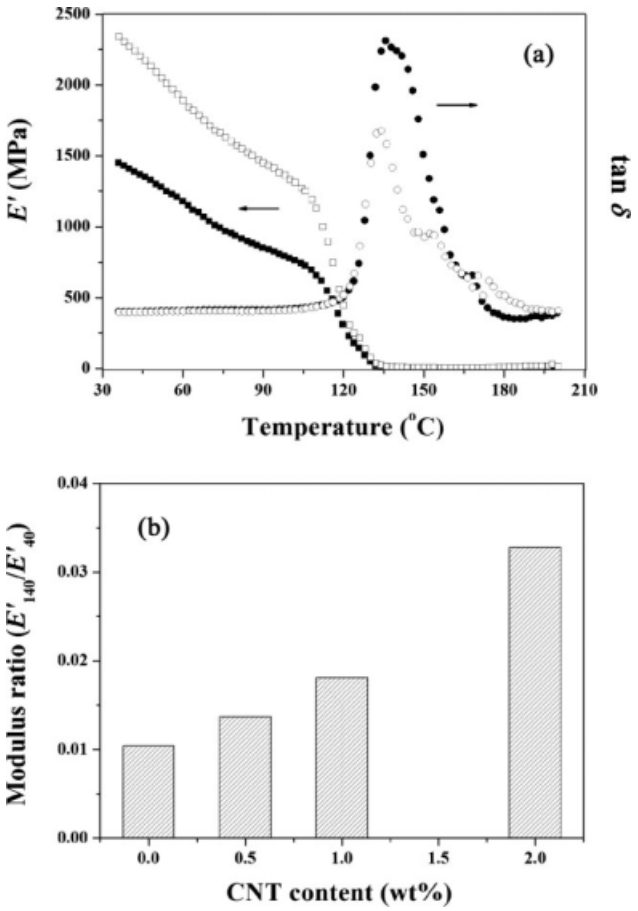

Figure 6 (a) Dynamic mechanical properties of PEN/CNT nanocomposites as a function of temperature [(●) PEN and (○) PEN/CNT 2.0 nanocomposites] and (b) modulus ratio of PEN/CNT nanocomposites with the CNT content.

of the storage modulus at 40°C (E'_{40}) for PEN/CNT nanocomposites to that at 140°C (E'_{140}) was estimated. As shown in Figure 6(b), the modulus ratio of the PEN/CNT nanocomposites increased with the introduction of CNTs. The incorporation of CNTs into the PEN matrix increased E' of PEN/CNT nanocomposites below and above the glass-transition region because of the nanoreinforcing effect of CNTs dispersed in the PEN matrix, thus enabling PEN/CNT nanocomposites to maintain high modulus values at elevated temperatures in comparison with PEN.

CONCLUSIONS

Polymer nanocomposites based on PEN and a small quantity of CNTs were prepared by simple melt compounding with a twin-screw extruder, and the effects of CNTs on the thermal stability and thermal decomposition kinetics of PEN/CNT nanocomposites were examined. A small quantity of CNTs in the PEN matrix could effectively enhance the

thermal stability of PEN/CNT nanocomposites. The thermal decomposition kinetics of PEN/CNT nanocomposites strongly depended on the CNT content, heating rate, and gas atmosphere. On the basis of thermal decomposition kinetic analyses, including Flynn–Wall–Ozawa, Kissinger, and Kim–Park methods, the variations of E_a of PEN/CNT nanocomposites confirmed that the incorporation of a small quantity of CNTs into the PEN matrix enhanced the thermal stability of PEN/CNT nanocomposites. The morphological observations revealed the formation of interconnected or network-like structures of CNTs in the PEN matrix, which may have stabilized PEN/CNT nanocomposites as thermal insulating layers during thermal decomposition. The dispersed CNTs played a critical role in improving the thermal stability and thermal decomposition characteristics of PEN/CNT nanocomposites by acting effectively as physical barriers against thermal decomposition. This study suggested that CNTs could be beneficial, acting as effective thermal-decomposition-resistant nanoreinforcing fillers in PEN/CNT nanocomposites. In addition, the introduction of CNTs increased E' of PEN/CNT nanocomposites and made it possible for them to sustain a higher modulus at elevated temperatures in comparison with pure PEN.

References

1. Ebbesen, T. W. Rev Mater Sci 1994, 24, 235.
2. Wong, E. W.; Sheehan, P. E.; Lieber, C. M. Science 1997, 277, 1971.
3. Bokobza, L. Polymer 2007, 48, 5279.
4. Kim, J. Y.; Kim, S. H. Polym Int 2006, 55, 449.
5. Kim, J. Y.; Kim, S. H. J Polym Sci Part B: Polym Phys 2005, 43, 3600.
6. Kim, J. Y.; Kim, S. H. J Appl Polym Sci 2006, 99, 2211.
7. Kim, J. Y.; Kim, S. H.; Kikutani, T. J Polym Sci Part B: Polym Phys 2004, 42, 395.
8. Pötschke, P.; Fornes, T. D.; Paul, D. R. Polymer 2002, 43, 3247.
9. Kumar, S.; Doshi, H.; Srinvasrao, M.; Park, J. O.; Schiraldi, D. A. Polymer 2002, 43, 1701.
10. Mu, M.; Walker, A. M.; Torkelson, J. M.; Winey, K. I. Polymer 2008, 49, 1332.
11. Kim, J. Y.; Park, H. S.; Kim, S. H. Polymer 2006, 47, 1379.
12. Kim, J. Y.; Kim, S. H. J Polym Sci Part B: Polym Phys 2006, 44, 1062.
13. Kim, J. Y.; Park, H. S.; Kim, S. H. J Appl Polym Sci 2007, 103, 1450.
14. Kim, J. Y.; Han, S. I.; Kim, S. H. Polym Eng Sci 2007, 47, 1715.
15. Kim, J. Y.; Han, S. I.; Hong, S. Polymer 2008, 49, 3335.
16. Kim, J. Y. J Appl Polym Sci 2009, 112, 2589.
17. Nair, C. P. R.; Bindu, R. L.; Joseph, V. C. J Polym Sci Part A: Polym Chem 1995, 33, 621.
18. Holland, B. J.; Hay, J. N. Polymer 2002, 43, 1835.
19. Park, S. J.; Cho, M. S. J Mater Sci 2000, 35, 3525.
20. Tang, W.; Li, X. G.; Yan, D. J Appl Polym Sci 2004, 91, 445.
21. Samperi, F.; Puglisi, C.; Alicata, R.; Montaudo, G. Polym Degrad Stab 2004, 83, 3.
22. Kashiwagi, T.; Du, F.; Douglas, J. F.; Winey, K. I.; Harris, R. H.; Shields, J. R. Nat Mater 2005, 4, 928.
23. Wang, H.; Meng, S.; Xu, P.; Zhong, W.; Du, Q. Polym Eng Sci 2007, 47, 302.
24. Kashiwagi, T.; Grulke, E.; Hilding, J.; Harris, R. H.; Awad, W.; Douglas, J. Macromol Rapid Commun 2002, 23, 761.
25. Bocchini, S.; Frache, A.; Camino, G.; Claes, M. Eur Polym J 2007, 43, 3222.
26. Watts, P. C. P.; Fearon, P. K.; Hsu, W. K.; Billingham, N. C.; Kroto, H. W.; Walton, D. R. M. J Mater Chem 2003, 13, 491.
27. Krusic, P. J.; Wasserman, E.; Keizer, P. N.; Morton, J. R.; Preston, K. F. Science 1991, 254, 1183.
28. Vyazovkin, S. Int Rev Phys Chem 2000, 19, 45.
29. Kissinger, H. E. J Anal Chem 1957, 29, 1072.
30. Ozawa, T. J Therm Anal 1970, 2, 301.
31. Hsiue, G. H.; Liu, Y. L.; Liao, H. H. J Polym Sci Part A: Polym Chem 2001, 39, 986.
32. (a) Ozawa, T. Bull Chem Soc Jpn 1965, 38, 1881; (b) Flynn, J. H.; Wall, L. A. Polym Lett 1966, 4, 323.
33. Doyle, C. D. J Appl Polym Sci 1962, 6, 639.
34. Kim, S.; Park, J. K. Thermochim Acta 1995, 264, 137.
35. Li, F.; Xu, X.; Li, Q.; Zhang, H.; Yu, J.; Cao, A. Polym Degrad Stab 2006, 91, 1685.
36. Wang, D. Y.; Wang, Y. Z.; Wang, J. S.; Chen, D. Q.; Zhou, Q.; Yang, B.; Li, W. Y. Polym Degrad Stab 2005, 87, 171.
37. Zhao, H.; Wang, Y. Z.; Wang, D. Y.; Wu, B.; Chen, D. Q.; Wang, X. L.; Yang, K. K. Polym Degrad Stab 2003, 80, 135.
38. Day, M.; Cooney, J. D.; Wiles, D. M. J Appl Polym Sci 1989, 38, 323.
39. Schartel, B.; Pötschke, P.; Knoll, U.; Abdel-Goad, M. Eur Polym J 2005, 41, 1061.
40. Moniruzzman, M.; Winey, K. I. Macromolecules 2006, 39, 5194.
41. (a) Berber, S.; Kwon, Y. K.; Tomanek, D. Phys Rev Lett 2000, 84, 4614; (b) Benedict, L. X.; Lourie, S. G.; Cohen, M. L. Solid State Commun 1996, 100, 177.
42. Huxtable, S. T.; Cahill, D. G.; Shenogin, S.; Xue, L.; Ozik, R.; Barone, P.; Usrey, M.; Strano, M. S.; Siddons, G.; Shim, M.; Keblinski, P. Nat Mater 2003, 2, 731.